periodica polytechnica

Transportation Engineering
41/2 (2013) 99–103
doi: 10.3311/PPtr.7109
http://periodicapolytechnica.org/tr

RESEARCH ARTICLE

Gigacycle Fatigue Endurance of Marine Grade Stainless Steels with Corrosion Pits

František Nový / *Viera* Zatkalíková / *Otakar* Bokůvka / *Katarína* Miková

Received 2013-09-04

Abstract

The fatigue resistance of commercial AISI 316L and AISI 316Ti austenitic stainless steels after corrosion attack by aggressive chloride-containing environment was examined with the aim to explore the influence of pitting corrosion on their fatigue resistance. The fatigue resistance after corrosion attack was found to be significantly reduced due to the occurrence of corrosion pits on the surface of tested specimens. The obtained results were compared with results predicted using empirical model given by Murakami. It was found that the fatigue limit of the tested steels with pitting corrosion, predicted according to empirical model proposed by Murakami, is much higher than real fatigue limit experimentally determined.

Keywords

Pitting corrosion · Chloride-containing environments · Austenitic stainless steel · Fatigue resistance

Acknowledgement

The research was partially supported by the Scientific Grant Agency of the Ministry of Education, Science and Sports of the Slovak Republic and Slovak Academy of Sciences, grant No. 1/0743/12, No. 1/0831/13 and by European regional development fund and Slovak state budget by the project ITMS 26220220048 (call OPVaV-2008/2.2/01-SORO).

František Nový
Department of Materials Engineering, University of Žilina,
Univerzitná 1, 010 26 Žilina, Slovak Republic
e-mail: frantisek.novy@fstroj.uniza.sk

Viera Zatkalíková
Department of Materials Engineering, University of Žilina,
Univerzitná 1, 010 26 Žilina, Slovak Republic

Otakar Bokůvka
Department of Materials Engineering, University of Žilina,
Univerzitná 1, 010 26 Žilina, Slovak Republic
e-mail: otakar.bokuvka@fstroj.uniza.sk

Katarína Miková
Department of Materials Engineering, University of Žilina,
Univerzitná 1, 010 26 Žilina, Slovak Republic

1 Introduction

Marine grade stainless is a stainless steel preferred for use in marine environments to avoid pitting corrosion. The family of AISI 316 (316, 316L, 316N, 316Ti, 316H) steels is known as "marine grade" stainless steels due to their increased ability to resist saltwater corrosion compared to type AISI 304.

Grade 316 is the standard molybdenum-bearing grade, second in importance to 304 amongst the austenitic stainless steels. The molybdenum gives 316 better overall corrosion resistant properties than grade 304, particularly higher resistance to pitting and crevice corrosion in chloride environments. Grade 316L, the low carbon version of 316 and is immune from sensitisation (grain boundary carbide precipitation). Thus it is extensively used in heavy gauge welded components (over about 6 mm). Grade 316H, with its higher carbon content has application at elevated temperatures (particularly at temperatures above about 500°C), as does stabilised grade 316Ti, but should not be used for applications where sensitisation corrosion could be expected.

Grade 316 has excellent corrosion resistance in a wide range of media. Its main advantage over grade 304 is its increased ability to resist pitting and crevice corrosion in warm chloride environments. In hot chloride environments, grade 316 is subject to pitting and crevice corrosion and to stress corrosion cracking when subjected to tensile stresses beyond about 50°C. The corrosion resistances of the low (316L, 316N) and high (316Ti, 316H) carbon versions of 316, are the same as standard 316 (Fajnor [4]). They are mostly chosen to give better resistance to sensitisation in welding (316L, 316Ti) or for superior high temperature strength (316H).

In addition to marine the 316 steel is often used in the chemical industry, apparatus engineering, sewage plants, and paper industry, nuclear reprocessing plants and in the handling of certain food and pharmaceutical products where it is often required in order to minimize metallic contamination. It is resistant to most food processing environments, organic chemicals, dye stuffs and a wide variety of inorganic chemicals. And it has excellent forming and welding characteristics (Liptáková [7], Žarnay [14]).

Resistance to pitting and crevice corrosion is very important if the steel is to be used in chloride-containing environments.

Austenitic stainless steels show a very high corrosion resistance in many aggressive environments, nevertheless they can suffer pitting corrosion in chloride ion rich solutions (Szklarska-Smialowska [12], Teoh [13]). Austenitic steels are more or less resistant to general corrosion, crevice corrosion and pitting corrosion, depending on the quantity of alloying elements. Resistance to pitting and crevice corrosion increases with increasing contents of chromium, molybdenum and nitrogen (Hadzima, et al [5]). For stainless steels the influence of pitting corrosion at the critical part under cyclic loading is not negligible and it is of practical importance (ASM Handbook [1], Khatak et al. [6]). This problem is very difficult fatigue problem, and is not easy solved. It has not previously been sufficiently studied because of the complicated phenomena and complicated testing. However, a quantitative solution of this problem is very much needed, because the loads applied to components and structures are being raised year by year. High cycle fatigue has become a major concern in design and durability of engineering components and structures. This concern has led to increased research activities in high cycle fatigue, including basic understanding of failure mechanisms, development of new experimental techniques, analysis methods, and life prediction methods. The S-N (stress-cycles) curve is often still assumed to be a rectangular hyperbolic relationship, but in reality there is not a horizontal asymptote. This means that fatigue initiation mechanisms from 10^6 to beyond 10^9 cycles are a topic of great interest for advanced structural technologies. Consequently the S-N curve, since it is not asymptotic, must be determined in order to guarantee the real fatigue strength in the very high cycle regime. It has been generally accepted that at high stress levels, fatigue life is determined primarily by crack growth, while at low stress levels, the life span is mainly consumed by the process of crack initiation. Several authors have demonstrated that the portion of life attributed to crack nucleation is above 90% in the high-cycle regime (10^6 to 10^7 cycles) for steel, aluminium, titanium, and nickel alloys. In the very high cycle and ultra high cycle regime the ratio between crack nucleation period and crack growth period is more than 99.99 : 0.01. To reach 10^9 cycles using conventional fatigue testing machine working at 50 Hz will take 230 days, which is very time consuming and expensive. A possibility of accelerated fatigue testing is now considered by using high frequency (ultrasonic) cyclic loading. The ultrasonic fatigue test method differs from the conventional fatigue test method that has frequency limited to 200 Hz of cyclic stressing of material. The frequency of ultrasonic fatigue testing ranges from 15 kHz to 40 kHz, with a typical frequency being 20 kHz. With this high frequency, the time and cost to obtain a fatigue limit or crack growth rate threshold data can be dramatically reduced (Bokůvka et al. [3]). This work deals with the influence of pitting corrosion of two most corrosion resistant stainless steels on their fatigue resistance in gigacycle region.

2 Material and experimental

Commercial AISI 316L and AISI 316Ti stainless steels were used as an experimental material. Experimental material was supplied in rolled sticks with diameter 12 mm, in cold drawn condition.

The mechanical properties and chemical composition are given in Tables 1 and 2. The microstructure is shown in Fig. 1 and 2.

Tab. 1. Mechanical properties of AISI 316L and AISI 316Ti steels

Steel type	R_e [MPa]	R_m [MPa]	A_5 [%]	Z [%]	$HV_{10/10}$
AISI 316L	248	753	53	46	246
AISI 316Ti	251	773	54	48	213

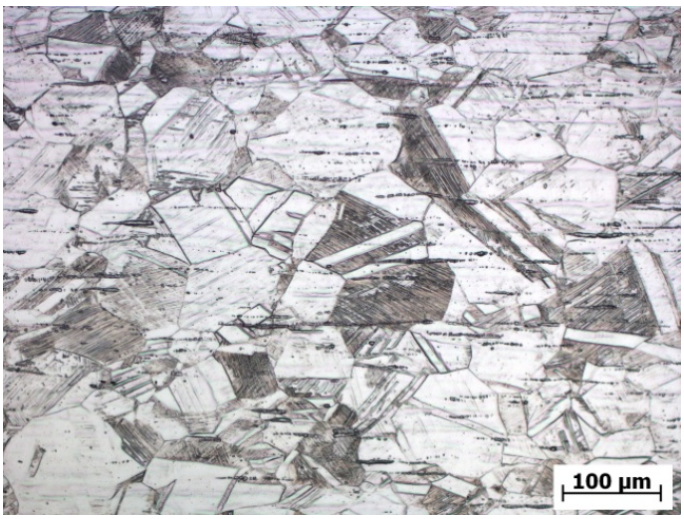

Fig. 1. Microstructure of AISI 316L steel

Metalographic specimens for microstructure analysis were taken out in longitudinal direction to consider influence of processing technology on final microstructure. Specimens were prepared by standard metallographic procedures and were etched by mixture of acids and glycerine (10 ml HNO_3, 30 ml HCL, 20 ml glycerine) by virtue of the fact, that stainless steels are highly corrosion resistant, and very strong acids are required to reveal their microstructure.

Tab. 2. Chemical composition of AISI 316L and AISI 316Ti steels

Steel type	**C**	**Cr**	**Ni**	**Mo**	**Mn**
AISI 316L	0.026	17.32	13.68	2.73	1.89
AISI 316Ti	0.058	17.55	12.96	2.54	1.63
Steel type	**Si**	**S**	**P**	**Ti**	**Fe**
AISI 316L	0.65	0.026	0.028	0.002	balance
AISI 316Ti	0.81	0.037	0.033	0.371	balance

Microstructure (described properly in (Nový et al. [11]) is formed by inhomogeneous grains of austenite, delta ferrite, carbonitrides of titanium, and carbides of alloying elements. Colonies of delta ferrite and carbonitrides are arranged on lines

Fig. 2. Microstructure of AISI 316L steel

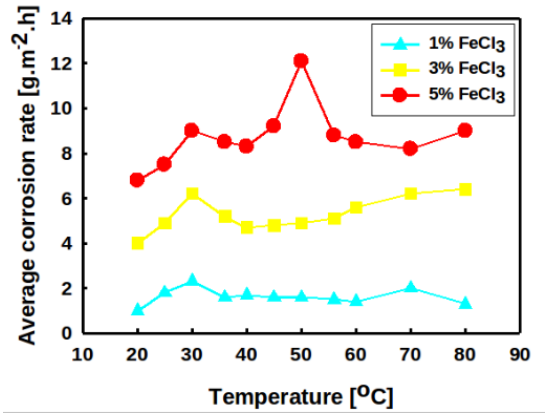

Fig. 3. Dependence of the average corrosion rate on temperature for 1, 3 and 5% $FeCl_3$ solution; AISI 316Ti steel

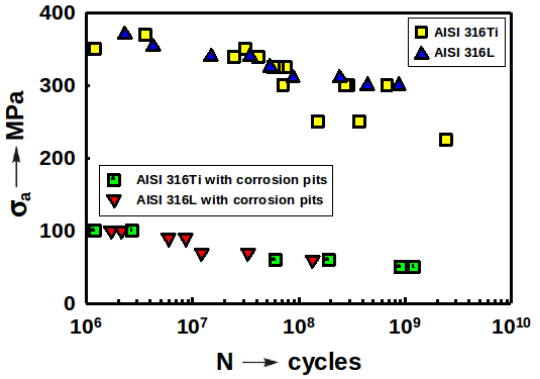

Fig. 4. The S-N curves of AISI 316L and AISI 316Ti steels

as a result of cold-rolling. Carbides and carbonitrides are segregated mainly inside of austenite grains, or in the vicinity of grain boundary. For austenite grains is typical countless amounts of deformation and annealing twins after cold working and annealing process, most of all in appropriable oriented grains according to direction of hot forming.

The corrosion attack was realized in chloride solution according ASTM G4 standard (Baboian et al. [2]). This standard is used for evaluation of resistance of stainless steel against pitting corrosion. Immersion tests were carried out in the 5% $FeCl_3$ solution (Cl- concentration of $0.9624\,\mathrm{mol}\times\mathrm{dm}^{-3}$) at the temperature 50°C. The duration of the mentioned test was 24 hours. After 24 hour exposure the specimens were carefully brushed, washed by demineralized water and freely dried up. These conditions were chosen according to results of previous corrosion tests of AISI 316 Ti steel in corrosion environments with various

Cl- concentrations (1, 3 and 5% $FeCl_3$ solution) at various temperatures (Fig. 3). The highest average corrosion rate in the temperature range from 20 to 80°C was recorded in 5% $FeCl_3$ (Fig. 3).

The significant changes of the corrosion rates are expression of changes of mechanism controlling the pitting corrosion. This change of corrosion mechanism means the changeover between combined and diffusive control of kinetics of pitting corrosion. The significant changeover from diffusive to combined control was recorded in the range of temperature from 40 to 50°C for 5% $FeCl_3$ solution. This change corresponds with change of appearance of surface of the specimens after corrosion attack. The density of corrosion pits rapidly increases and the size of corrosion pits decreases, but the depth of pits increases. The average density of corrosion pits about $17.3\,\mathrm{N}\times10^4\times\mathrm{m}^{-2}$ was recorded in the 5% $FeCl_3$ solution at the temperature 50°C for AISI 316 Ti. For AISI 316L the average density of corrosion pits was about $28.4\,\mathrm{N}\times10^4\times\mathrm{m}^{-2}$; measured using the same conditions as in case of AISI 316Ti steel. This type of corrosion attack was selected as a reference type of corrosion attack for investigation of influence of corrosion attack on fatigue endurance of studied steels.

Fatigue investigations were carried out under fully reversed axial loading (load ratio $R = -1$, frequency $f \approx 20$ kHz and ambient temperature) in the region from $N = 10^6$ to $N = 2\times10^9$ cycles using high-frequency resonant ultrasonic machine and smooth specimens.

3 Results and discussion

The results of fatigue tests were plotted as relation of stress amplitude vs. number of cycles to failure in Fig. 4.

The fatigue limit σ_c (at $N = 10^9$ cycles) of AISI 316L steel is $\sigma_c = 250$ MPa and in case of AISI 316Ti steel it is $\sigma_c = 300$ MPa. The significant effect of corrosion damage was recorded. Due to the corrosion attack was the fatigue limit reduced to the value of 65 MPa for both of the steels. Fatigue cracks initiated naturally at the microstructurally weakest points.

Surface crack initiation due to the formation of extrusion and intrusion during fatigue test was typical for the both steels (AISI 316L and AISI 316Ti) without corrosion damage. Crystallographic oriented initiation of fatigue crack was observed on all of the fatigue failured specimens without corrosion attack. On the other hand, after corrosion damage, both steels were charac-

teristic by fatigue crack initiation from the corrosion pits on the surface (Fig. 5).

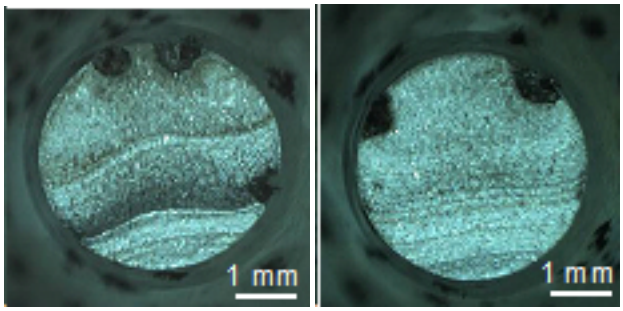

(a) AISI 316L (b) AISI 316Ti

Fig. 5. Fatigue fractures and corrosion pits

Fatigue lifetime in low, high and gigacycle regime is influenced by surface (notches, pits, dints, roughness, etc.) and subsurface defects (cavities, pores, shrinkages, inclusions, etc.). The most useful methods available to predict the fatigue limit stress of metals containing inclusions are based on the assumption that inclusions can be treated as cracks. Using these methods the inclusion could simply be associated with the notch effects on the matrix material. Than the fatigue limit corresponds to the cyclic stress at which these crack-like defects do not propagate. With regard to importance of given problem the approaches consider the influence of small defects, especially inclusions and small surface defects, like roughness and corrosion pits are in demand. One of the possibilities how to predict the fatigue lifetime is application of the empirical model $\sqrt{\text{area}}$, which Murakami proposed and presented in his works [Murakami[10], Murakami [8], Murakami [9]]. Empirical model $\sqrt{\text{area}}$ assuming a small surface defect being equivalent to a small crack is presented as follows:

$$\sigma_w = 1.43 \frac{(\text{HV} + 120)}{(\sqrt{\text{area}})^{\frac{1}{6}} [(1-R)/2]^{\alpha}} \qquad (1)$$

where σ_w is predicted fatigue limit, HV is Vickers hardness of the matrix (in the range of 100 - 740), R is stress ratio, coefficient $\alpha = 0.266 + \text{HV} \times 10^{-4}$, $\sqrt{\text{area}}$ is area of plan surface of maximal inclusion to the perpendicular direction to maximum tensile stress (Fig. 6). Based on mentioned hypothesis the experimental data obtained from tension-compression fatigue test were analysed by the empirical model $\sqrt{\text{area}}$, which has regard for failure of specimens on surface defects.

Predicted fatigue limit σ_w was determined by using hardness HV = 246 for AISI 316L and by using hardness HV = 213 for AISI 316Ti. In the Tables 3 and 4, the values of fatigue lifetime σ_a obtained by experimental fatigue tests are presented and these data are comparised with the estimated values of predicted fatigue limit σ_w.

If the value of stress amplitude σ_a around the corrosion pit is higher than the value of predicted fatigue limit, the corrosion pit becomes to be a fatigue failure initiator (Murakami [10]).

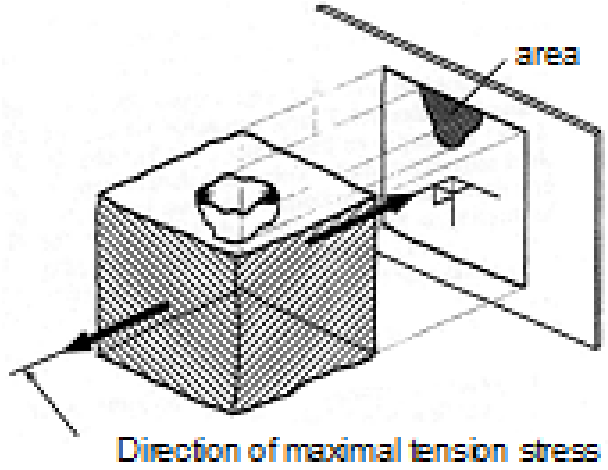

Fig. 6. Definition of $\sqrt{\text{area}}$

Tab. 3. Predicted fatigue limit for AISI 316L

σ_a [MPa]	$(\sqrt{\text{area}})^{\frac{1}{6}}$ [μm]	σ_w [MPa]	σ/σ_w
360	2.85	183	1.96
380	2.77	188	2.00
340	2.81	185	1.83
320	2.91	180	1.77
310	2.92	178	1.74

According to Murakami model the small defects are initiators of fatigue failure only when the σ_a/σ_w ratio is higher than 1. In this study, the σ_a/σ_w ratio exceeded this limit in all cases. Moreover, every corrosion pit observed on the surface of tested specimens can be assumed as fatigue crack formable. On the other hand, despite to this theory given by Murakami the predicted fatigue limit σ_w is much higher than the real fatigue limit, which was experimentally determined. The real fatigue limit of both of the tested steels after corrosion attack is less than the half of the predicted fatigue limit.

Tab. 4. Predicted fatigue limit for AISI 316Ti

σ_a [MPa]	$(\sqrt{\text{area}})^{\frac{1}{6}}$ [μm]	σ_w [MPa]	σ/σ_w
370	3.10	153	2.42
360	2.64	180	2.00
340	3.10	153	2.17
340	3.06	155	2.12
330	2.77	171	1.93

4 Conclusions

The fatigue resistance of AISI 316L and AISI 316Ti austenitic stainless steels after corrosion attack by aggressive chloride-containing environment was examined with the aim to explore the influence of pitting corrosion on their fatigue behaviour. The

obtained results were compared with results predicted using empirical model given by Murakami. With regard on the carried out experimental works the following conclusions can be summarized:

- the resistance against crack initiation is significantly reduced due to the corrosion pits occurrence on the surface of tested specimens,
- given the role of corrosion pits in the fatigue failures of tested steels, the corrosion pits could be directly associated with the origin of the crack,
- the shape, size and quantity of corrosion pits are factors controlling the fatigue resistance,
- the fatigue limit of the tested steels with pitting corrosion, predicted according to empirical model $\sqrt{\text{area}}$ proposed by Murakami is much higher than real fatigue limit experimentally determined.

References

1 *ASM Handbook, Corrosion*, 4th, ASM International, 1992.

2 **Baboian R, et al.**, *Corrosion Test and Standards*: *Application and Interpretation*, ASTM Manual Series, ASTM International, 1995.

3 **Bokůvka O, Nový F, Chalupová M, Nicoletto G**, *Gigacycle Fatigue at High-frequency Loading*, Diagnostyka, **48**(4), (2008), 53–56.

4 **Fajnor P, Liptáková T**, *Surface state effect on pitting corrosion of the AISI 316Ti*, International Journal of Applied Mechanics and Engineering, **14**, (2004), 1009–1014.

5 **Hadzima B, Liptáková T**, *Základy elektrochemickej korózie kovov*, EDIS ŽU; Žilina. (in Slovak), 2008.

6 **Khatak HS, RAJ B**, *Corrosion of Austenitic Stainless Steels, Mechanism, Mitigation and Monitoring*, ASM International; Ohio, 2002.

7 **Liptáková T**, *Bodová korózia nehrdzavejúcich ocelí*, EDIS ŽU; Žilina. (in Slovak), 2009.

8 **Murakami Y, Kodama S, Konuma S**, *Quantitative evaluation of effects of non-metallic inclusions on fatigue strength of high strength steels. I.*: *I: Basic fatigue mechanism and evaluation of correlation between the fatigue fracture stress and the size and location of non-metallic inclusions*, International Journal of Fatigue, **11**(Issue 5 September), (1989), 291–298.

9 **Murakami Y, Usuki H**, *Quantitative evaluation of effects of non-metallic inclusions on fatigue strength of high strength steels. II.*: *II: Fatigue limit evaluation based on statistics for extreme values of inclusion size*, International Journal of Fatigue, **11**(Issue 5 September), (1989), 299–307.

10 **Murakami Y**, *Metal Fatigue*: *Effect of Small Defects and Non-metallic Inclusions*, Elsevier, 2002.

11 **Nový F, Bokůvka O, Chalupová M, Motýľová E**, *Fatigue Resistance of AISI 316L and AISI316Ti Steels*, Materials Engineering, **15**(2a), (2008), 79–84.

12 **Szklarska-Smialowska Z**, *Pitting and Crevice Corrosion*, NACE International; Houston, Texas, 2005.

13 **Teoh SH**, *Fatigue of Biomaterials*: *a Review*, International Journal of Fatigue, **22**(10), (2000), 825–837.

14 **Žarnay M, Bronček J, Ľahučký D.**, *Design engineer and competitiveness of the product*, Produktywność i Innowacje, **6**(3), (2007), 17–21.